

Published in final edited form as:

Biochim Biophys Acta. 2011 July ; 1808(7): 1818–1826. doi:10.1016/j.bbame.2011.03.004.

Cpt-cAMP activates human epithelial sodium channels *via* relieving self-inhibition

Raul Molina^{a,#}, Dong-Yun Han^{a,#}, Xue-Feng Su^a, Run-Zhen Zhao^a, Meimi Zhao^a, Gretta M. Sharp^a, Yongchang Chang^c, and Hong-Long Ji^{a,b}

^a Department of Biochemistry, University of Texas Health Science Center at Tyler, TX, USA

^b Texas Lung Injury Institute, University of Texas Health Science Center at Tyler, TX, USA

^c Division of Neurobiology, Barrow Neurological Institute, St Joseph's Hospital and Medical Center, AZ, USA

Abstract

External Na⁺ self-inhibition is an intrinsic feature of epithelial sodium channels (ENaC). Cpt-cAMP regulates heterologous guinea pig but not rat $\alpha\beta\gamma$ ENaC in a ligand-gated manner. We hypothesized that cpt-cAMP may eliminate the self-inhibition of human ENaC thereby open channels. Regulation of self-inhibition by this compound in oocytes was analyzed using the two-electrode voltage clamp and Ussing chamber setups. External cpt-cAMP stimulated human but not rat and murine $\alpha\beta\gamma$ ENaC in a dose- and external Na⁺ concentration-dependent fashion. Intriguingly, cpt-cAMP activated human $\delta\beta\gamma$ more potently than $\alpha\beta\gamma$ channels, suggesting that structural diversity in ectoloop between human α , δ , and those ENaC of other species determines the stimulating effects of cpt-cAMP. Cpt-cAMP increased the ratio of stationary and maximal currents. Mutants having abolished self-inhibition ($\beta_{\Delta V348}$ and γ_{H233R}) almost completely eliminated cpt-cAMP mediated activation of ENaC. On the other hand, mutants both enhancing self-inhibition and elevating cpt-cAMP sensitivity increased the stimulating effects of the compound. This compound, however, could not activate already fully opened channels, *e.g.*, degenerin mutation ($\alpha\beta_{S520C\gamma}$) and the proteolytically cleaved ENaC by plasmin. Cpt-cAMP activated native ENaC to the same extent as that for heterologous ENaC in human lung epithelial cells. Our data demonstrate that cpt-cAMP, a broadly used PKA activator, stimulates human $\alpha\beta\gamma$ and $\delta\beta\gamma$ ENaC channels by relieving self-inhibition.

1. Introduction

Epithelial Na⁺ channels (ENaC) are an apically located critical pathway for reabsorbing salt from luminal solution [1–3]. ENaC may serve as a ligand-gated channel and regulated by external compounds [2, 4]. These compounds include *para*-chloromercuribenzoate [2], benzimidazolyl-2-guanidinium [2], protons [5–7], Cl[−] [8], multivalent cations [9, 10], cpt-cAMP [11], 8-pCPT-cGMP [12], glibenclamide [13], gaseous halothane [14], bumetanide [15], and a small molecule S6939 [16]. Among them, some have been reported to abolish

© 2011 Elsevier B.V. All rights reserved.

Correspondence: Hong-Long Ji, University of Texas Health Science Center at Tyler, 11937 US Highway 271, Tyler, TX 75708-3154, james.ji@uthct.edu.

[#]These authors equally contribute to the manuscript

Publisher's Disclaimer: This is a PDF file of an unedited manuscript that has been accepted for publication. As a service to our customers we are providing this early version of the manuscript. The manuscript will undergo copyediting, typesetting, and review of the resulting proof before it is published in its final citable form. Please note that during the production process errors may be discovered which could affect the content, and all legal disclaimers that apply to the journal pertain.

external Na⁺ self-inhibition, an intrinsic phenomenon of ENaC, sensitive to temperature [2, 4, 5, 9, 17–19]. In sharp contrast, Collier and Snyder proved that extracellular chloride enhances this process and thereby inhibits ENaC in a pH-dependent manner [8]. In addition to ENaC, acid-sensing Na⁺ channels (ASIC), a branch of the ENaC/DEG super gene family, are gated by external protons [20]; and FaNaC channels are manipulated by FMRFamide and related tetrapeptides [21].

Cpt-cAMP, as a cell permeable specific PKA activator has long been used for studying epithelial Na⁺ channels. Chraïbi and colleagues found that the compound specifically activated guinea pig but not rat ENaC in oocytes [11]. Furthermore, a key responsive domain in guinea pig α subunit (Ile481) was identified [22]. Human ENaC responded to cpt-cAMP in a dose-dependent, time-independent, and reversible manner [23]. In addition to these heterologous channels, amiloride-sensitive, cpt-cAMP activated cation channels were also reported in human Clara cells (H441) and human lymphocytes in a similar manner [24–27]. To date, the interpretation for the acute activation of both native and heterologous human ENaC activity by cpt-cAMP is still limited to the mediation of PKA pathway.

A number of critical amino acid residues are involved in governing self-inhibition. Sheng and coworkers identified the cysteine and histidine residues in α and γ subunits were critical [28, 29]. Very recently, this group provided strong evidence that α Gly481 and γ Met438 resided in the thumb domain were functional determinants of self-inhibition [19]. In addition to the relief of self-inhibition, the external ligand-like compounds activated ENaC channels analog to serine proteases [30–32]. Our recent observations on the regulation of ENaC by 8-pCPT-cGMP are of supportive to this notion [12].

The aim of this study was to examine if cpt-cAMP relieves self-inhibition thereby to active human ENaC activity. We observed that this compound activates ENaC in a dose-dependent manner only when perfused to cell surface. Abrogation of self-inhibition in mutated channels eliminated the response to cpt-cAMP, while mutations amplifying self-inhibition enhanced the effects of cpt-cAMP. Furthermore, cpt-cAMP did not activate already fully opened channels by mutating degenerin site or protease exposure.

2. Materials and Methods

2.1 Site-directed and deletion mutagenesis

Wild type human α , β , γ , and δ ENaC cDNAs were a gift from Dr. Lingueglia [33]. Single point mutants were generated using the QuikChange site-directed mutagenesis kit (Stratagene, La Jolla, CA). All the mutants were confirmed by sequencing.

2.2 Oocyte expression and voltage clamp studies

Oocytes were surgically removed from appropriately anesthetized adult female *Xenopus laevis* (Xenopus Express) and cRNAs for full length and mutated α , β , and γ ENaC were prepared as described previously [34]. Briefly, the ovarian tissue was removed from frogs under anesthesia by ethyl 3-aminobenzoate methanesulfonate salt (Sigma) through a small incision in the lower abdomen. Ovary lobes were removed and digested in OR-2 calcium-free medium (in mM: 82.5 NaCl, 2.5 KCl, 1.0 MgCl₂, 1.0 Na₂HPO₄, and 10.0 HEPES, pH 7.5) with the addition of 2 mg/ml collagenase (Roche Indianapolis). Defolliculated oocytes were cytosolically injected with ENaC cRNAs (25 ng per oocyte in 50 nl of RNase free water) and incubated in half-strength L-15 medium at 18°C. The two-electrode voltage clamp technique was used to record whole-cell currents 48 h post injection. Oocytes were impaled with two electrodes filled with 3M KCl, having resistances of 0.5–2 M Ω . A TEV-200 voltage clamp amplifier (Dagan) was used to clamp oocytes with concomitant recording of currents. Two reference electrodes were connected to the bath. The

continuously perfused bathing solution was ND96 medium (in mM: 96.0 NaCl, 1.0 MgCl₂, 1.8 CaCl₂, 2.5 KCl, and 5.0 HEPES, pH 7.5). Whole-cell currents were recorded as previously reported [35]. Experiments were controlled by pCLAMP 10.1 software (Molecular Devices), and currents at -40 mV, -100 mV, and +80 mV were continuously monitored with data recorded at intervals of 10s. Data were sampled at the rate of 1,000 Hz and filtered at 500 Hz.

To study the self-inhibition, a low Na⁺ (1 mM) bath solution was used (95 mM Na⁺ in regular ND-96 medium was substituted with equal molar NMDG). 8-pCPT-cAMP (AXXORA, LLC, San Diego, CA) stock solution (50 mM) was prepared in water and stored at -20°C. MTSET (Toronto Research Chemicals, Downsview, ON, Canada) was freshly prepared every 10 minutes. To elicit self-inhibition, oocytes were held at -60 mV continuously while the bath solution was switched quickly between regular ND-96 and the low Na⁺ solutions, controlled with a SF-77B Perfusion Fast-Step System (Warner Ins.).

2.3 Human lung epithelial cell culture and Ussing chamber studies

H441 cells (ATCC) were cultured in air-liquid interface as described previously [36]. Confluent tight monolayers with high transepithelial resistance (>800 MΩ·cm²) were mounted on the vertical Ussing chambers (Physiologic Instrument). To prevent proteolytic cleavage of ENaC, protease inhibitor cocktail (2μg/ml, Roche) was added to culture medium 12 hrs prior to recording. Amiloride-sensitive short-circuit currents (ASI_{sc}) were compared between controls (saline treated) and monolayers preincubated with protease inhibitors.

2.5 Data analysis

All results were presented as mean ± S.E.M. Dose-response curves were fitted to the Hill equation. Student t-test or One-way ANOVA computations were used to analyze the difference of the means for normally distributed data. P<0.05 was considered significant.

3. Results

3.1 External but not internal cpt-cAMP acutely stimulates human ENaC in a dose-dependent manner

ENaC channels have been proposed to behave as ligand-gated cation channels and acutely activated by cpt-cAMP [2, 4]. Taking advantage of the PKA-independent regulation of heterologously expressed human ENaC in oocytes, we examined the effects of cpt-cAMP, either external perfusion or intraoocyte microinjection, on human αβγ ENaC in oocytes. Repeatedly delivery of three doses (0.2 mM) of cpt-cAMP into cytosol did not alter the current level (Fig. 1A). Subsequent superfusion of the drug (0.2 mM), in striking contrast, to the same cell rapidly evoked the current approximately 2 fold (Fig. 1A & B). Both basal and elevated currents were sensitive to amiloride. This stimulatory effect of cpt-cAMP depended on external Na⁺ content. Substitution of bath Na⁺ ions with impermeable cationic molecule-NMDG markedly eliminated the action of ENaC by the compound (Fig. 1C). These results suggest that cpt-cAMP significantly stimulates human αβγ ENaC activity only when applied extracellularly. Furthermore, by fitting the experimental data to the Hill equation (Fig. 1D), an EC₅₀ value of 49.0 ± 14 μM was calculated, with a Hill coefficient constant of 0.6 ± 0.08 (n=5, R²=0.997). Application of cpt-cAMP more than 2 mM, however, dramatically reduced ENaC currents (not shown). The concentration-effect relationship was diminished when oocytes were perfused with the bath solution containing 1 mM Na⁺ ions (n=13). Obviously, external cpt-cAMP activates αβγ ENaC in a dose- and external Na⁺ content-dependent manner.

In addition, divergent responses were observed among human, rat, and mouse ENaCs (Fig. 1E). The same dose (0.2 mM) of cpt-cAMP caused a significant increment in human (82%, $P < 0.05$ vs basal level) but not rat (17%) and mouse ENaC activities (15%).

3.2 Enhanced responses of human $\delta\beta\gamma$ ENaC to cpt-cAMP

Both α and δ ENaC are detected in human epithelial cells biochemically and physiologically, including airway, pneumocytes, and pleural mesothelia [37–39]. Although several stoichiometric models have been proposed for ENaC channels, including $3\alpha3\beta3\gamma$, $2\alpha1\beta1\gamma$, and $1\alpha1\beta1\gamma$, it appears that the biophysical features of channels do not depend on the architecture of channels, and that the crystal structure of ENaC has not been reported to date [40–46]. However, δ ENaC conferred the biophysical properties of $\alpha\beta\gamma$ channels and formed channels with a unitary Na^+ conductance of 8 pS, in agreement with that of neither $\alpha\beta\gamma$ (4 pS) nor $\delta\beta\gamma$ channels (12 pS) [37]. To compare the responses of human $\alpha\beta\gamma$, $\delta\beta\gamma$, and $\alpha\beta\gamma\delta$ channels to cpt-cAMP, we examined the concentration dependence (Fig. 2). Again, cpt-cAMP stimulated human $\alpha\beta\gamma$ ENaC in a dose-dependent manner (Fig. 2A). Intriguingly, $\delta\beta\gamma$ but not $\delta\alpha\beta\gamma$ currents rose to a relatively greater level at 1 mM (Fig. 2B & C). The EC_{50} values for $\delta\alpha\beta\gamma$ channels were $30.2 \pm 1.2 \mu\text{M}$, similar to that of $\alpha\beta\gamma$ (Fig. 2A). The EC_{50} value for $\delta\beta\gamma$ ENaC, however, cannot be computed precisely due to unsaturated dose of the compound. The solubility of sodium salt of cpt-cAMP and a potential increase of external Na^+ concentration limited us to apply higher doses to $\delta\beta\gamma$ ENaC. As predicted by the available experimental data for $\delta\beta\gamma$ ENaC, a dose >100 mM is required to obtain the saturated effects of cpt-cAMP. Although the basal ENaC activity of $\delta\alpha\beta\gamma$ ENaC was greater than those of $\alpha\beta\gamma$ and $\delta\beta\gamma$ channels (Fig. 2A–C), the current ratio between that measured at 1mM and the basal level before perfusion of cpt-cAMP was greatest for $\delta\beta\gamma$ ENaC (Fig. 2D).

3.3 Response to cpt-cAMP of “loss-of-self-inhibition” mutants

We postulated that the “loss-of-self-inhibition” mutants might not be activated by cpt-cAMP if cpt-cAMP activates ENaC through relieving self-inhibition. As shown in Fig. 3A & B, the whole-cell Na^+ currents associated with two “loss-of-self-inhibition” mutants ($\beta_{\Delta V348}$ and γ_{H233R}) were not activated by cpt-cAMP in contrast to wild type $\alpha\beta\gamma$ (Fig. 3B & C). Furthermore, we analyzed self-inhibition of $\beta_{\Delta V348}$ and γ_{H233R} channels (Fig. 4). Cpt-cAMP increased the current levels (I_{30s}) measured 30 seconds post switching bath solution to ND-96 medium of wild type but not mutated channels (Fig. 4A & B). The corresponding current ratio associated with the mutated channels was not increased compared with wild type channels (Fig. 4C).

3.4 Responses of “gain-of-self-inhibition” mutants to cpt-cAMP

In contrast to the “loss-of-self-inhibition” mutants, mutants reported to enhance self-inhibition might facilitate the up-regulation of ENaC by cpt-cAMP [19]. To explore this possibility, the increment in both maximal (I_{max}) and I_{30s} currents in cells expressing two self-inhibition boosting mutants, termed α_{Y458A} and γ_{M432G} , and both, was examined (Fig. 5A). Above a 2 fold increase was observed for mutated channels post cpt-cAMP perfusion for both I_{max} and I_{30s} levels (Fig. 5B, $P < 0.05$).

3.5 Responses of human cpt-cAMP domain mutation (α_{S483I}) to cpt-cAMP

An amino acid residue in the ectoloop of guinea pig α ENaC (I481) was critical for cpt-cAMP to active ENaC and conferred the response of rat counterpart [22]. We hypothesized that the substitution of serine (S483) at the same position in human α counterpart with isoleucine might augment the stimulatory effect of cpt-cAMP. Indeed, cpt-cAMP significantly evoked both I_{max} and I_{30s} levels of α_{S483I} (Fig. 6A & B). Furthermore, we co-

expressed this mutant with γ_{M432G} , a “gain-of-self-inhibition” mutant to examine the potential co-ordination in facilitating the stimulatory effects of cpt-cAMP. Both I_{max} and I_{30s} levels were greater than that of α_{S483I} alone (Fig. 6B). These observations indicate that substitution of serine with isoleucine enhances self-inhibition, which in turn, favors the stimulation of ENaC by cpt-cAMP.

3.6 Cpt-cAMP does not activate fully opened channels

Both native and heterologously expressed ENaC could be activated by serine proteases following proteolytic cleavage of ectoloop [30, 31, 47, 48]. There is a pool of uncleaved or partially cleaved channels at the cell surface that are inhibited by external Na^+ ions. Proteases (*e.g.*, trypsin) increase the channel activity and render them relatively insensitive to external Na^+ signal. This raised a new issue that cpt-cAMP may regulate ENaC by increasing channel open time. Thus, the response to cpt-cAMP of a maximally opened mutant, termed β_{S520C} , was examined before and after application of MTSET, a thiol modifying reagent used to lock each channel at its full open state (Fig. 7A). Before addition of MTSET, cpt-cAMP reversibly increased the current at -100 mV approximately 2 fold from $-1,515 \pm 255$ to $-2,913 \pm 561$ nA (Fig. 7B, $P < 0.01$). Subsequent perfusion of MTSET increased the basal current to $-8,555 \pm 1370$ nA (5.6 fold of basal current, $P < 0.001$). The same dose of cpt-cAMP did not affect currents in MTSET-exposed cells (Fig. 7A & B). The cpt-cAMP activated currents were significantly lesser than that in the absence of MTSET (Fig. 7C, $P < 0.001$).

Alternatively, we tested the effects of cpt-cAMP on fully opened channels in cells exposed to protease-plasmin [49–51]. Neither total currents nor stationary over maximal current ratio was altered by cpt-cAMP (Fig. 8). Taken together with the results in MTSET pretreated cells (Fig. 7), cpt-cAMP may eventually lead to an increment in channel activity *via* increasing open time.

3.8 Cleavage abolishes cpt-cAMP-mediated ENaC activation in human lung epithelial cells

To corroborate the findings in oocytes, we evaluated the effects of cpt-cAMP on native ENaC in human lung epithelial cells (H441 monolayers), in which biochemically and physiologically detectable ENaCs were evoked by cpt-cAMP [24]. Cpt-cAMP activated amiloride-inhibitable I_{sc} levels by approximately 8% (Fig. 9A, left panel), which was much lesser than that for cloned ENaC in oocytes (2 fold). It is possible that ENaC proteins in carcinoma H441 cells probably have been cleaved by overexpressed proteases [52, 53]. We thus incubated cells with protease inhibitors for 12 hrs. As anticipated, cpt-cAMP increased I_{sc} level up to 2-fold in cells pretreated with protease inhibitors (Fig. 9B & C).

4. Discussion

Cyclic AMP and its catalogs, particularly the cell permeable compounds, are designed to modulate cAMP-PKA signal pathway. Native ENaC channels were found to be activated by cell permeable cpt-cAMP in pneumocytes [24, 54], endometrium [55], cortical collecting epithelium [56], and peripheral blood lymphocytes [25]. Heterologous ENaC activity was also augmented by cpt-cAMP in MDCK and oocytes [23, 57, 58]. The following evidence provides a novel mechanism for cpt-cAMP mediated acute activation of both heterologous and native human ENaC channels. First, external but not internal cpt-cAMP activates ENaC in seconds in a dose-dependent and reversible manner. Second, the specific chlorophenylthio (cpt) groups are required but not other more specific PKA activators with more potency in cell permeability [12]. Third, cpt-cAMP may not recruit new channel proteins to increase electrically detectable channel density at cell surface, as the stimulatory effects were also observed in outside-out patches, a cell-free model without functional machinery for

exocytosis, by our and other groups [12, 22]. Forth, mutations both enhancing and eliminating self-inhibition affect the effects of cpt-cAMP on ENaC. Fifth, self-inhibition modifying maneuvers, including proteolytic cleavage and thiol modification, prevent the cpt-cAMP-mediated activation.

So far, the identified critical amino acid residues in each subunit, which either boost (*i.e.*, α_{Y458} , γ_{M432}) or abolish (*i.e.*, α_{W493} , $\beta_{\Delta V348}$, γ_{H233}) self-inhibition, reside in extracellular finger, thumb, and palm domains and are the superficial domains of complexes. The location of these domains determines the susceptibility to cpt-cAMP. We cannot, however, conclude that cpt-cAMP directly modifies these self-inhibition domains, for the fact that external binding sites for H^+ and Cl^- ions in crystallized structure of ENaC/DEG proteins [5, 8], which also interrupt self-inhibition, locate differently. Because the unitary conductance was not altered by cpt-cAMP, the Na^+ conduction sites of ENaC seem not be modified. Self-inhibition appears initiated from external finger and thumb domains, palm domains are involved in secondarily conducting the signal of Na^+ concentration. The three-dimensional structural alteration of palm domains may subsequently result in the process of inactivation of channel gating. Eventually channel activity is reduced. Although we do not know if the self-inhibition modifying reagents augment the Na^+ binding and gating processes, which has not been understood yet so far, it is conceivable to infer that cpt-cAMP and other compounds may be capable of down-regulating the transition of Na^+ signal and resultant gating kinetics.

Few channel proteins, including cyclic nucleotide-gated channels (CNG), contain intracellular nucleotide-binding domains (NBD) [59]. It is worthy to note that these NBD domains do not require for specific structures of nucleotides, even the parental compounds, *e.g.*, cAMP and cGMP, can bind to the channel proteins [59]. Requirement of specific *cpt* groups in cAMP analogs to activate ENaC implies that cpt-cAMP may not dock into an external site with similar three-dimensional structure to NBD domains. Further studies are required to identify the docking site for cpt-cAMP and other analogs.

Domains in the extracellular loop in human δ ENaC facilitate activation of ENaC by cpt-cAMP *via* unknown mechanisms. These domains may form a more efficient pocket for cpt-cAMP binding, but our dose-response data do not support this notion. The estimated EC_{50} value of $\delta\beta\gamma$ ENaC is apparently much greater than those for $\alpha\beta\gamma$ and $\delta\alpha\beta\gamma$ channels (Fig. 2). Diversities in extracellular loop may also contribute to the species-dependent responses to cpt-cAMP.

The relief of self-inhibition by cpt-cAMP contributes to the acute effects, in addition to the well-known cAMP-PKA signal pathway. Although cpt-cAMP is not a natural endogenous cellular signal molecule, and the EC_{50} values are much greater than that for activating PKA, without doubt, it can be delivered into epithelial organs, such as alveolar spaces, as a potent pharmaceutical maneuver to acutely release edematous disorders. The clinical relevance, in fact, has been implicated in the up-regulation of ENaC in autosomal recessive pseudohypoaldosteronism type 1 (PHA-1) [25] and edematous lung injury [24].

Acknowledgments

The authors are grateful of suggestive discussion with Dr. Mark Atkinson and Ms. Deepa Bhattarai. This work was supported by NIH grants HL87017 and HL095435.

References

1. Garty H. Regulation of the epithelial Na^+ channel by aldosterone: open questions and emerging answers. *Kidney Int.* 2000; 57:1270–1276. [PubMed: 10760053]

2. Garty H, Benos DJ. Characteristics and regulatory mechanisms of the amiloride-blockable Na⁺ channel. *Physiol Rev.* 1988; 68:309–373. [PubMed: 2451832]
3. Rossier BC, Pradervand S, Schild L, Hummler E. Epithelial sodium channel and the control of sodium balance: interaction between genetic and environmental factors. *Annu Rev Physiol.* 2002; 64:877–897. [PubMed: 11826291]
4. Horisberger JD, Chraibi A. Epithelial sodium channel: a ligand-gated channel? *Nephron Physiol.* 2004; 96:p37–41. [PubMed: 14988660]
5. Collier DM, Snyder PM. Extracellular protons regulate human ENaC by modulating Na⁺ self-inhibition. *J Biol Chem.* 2009; 284:792–798. [PubMed: 18990692]
6. Ji HL, Benos DJ. Degenerin sites mediate proton activation of deltatetagamma-epithelial sodium channel. *J Biol Chem.* 2004; 279:26939–26947. [PubMed: 15084585]
7. Yamamura H, Ugawa S, Ueda T, Nagao M, Shimada S. Protons activate the delta-subunit of the epithelial Na⁺ channel in humans. *J Biol Chem.* 2004; 279:12529–12534. [PubMed: 14726523]
8. Collier DM, Snyder PM. Extracellular chloride regulates the epithelial sodium channel. *J Biol Chem.* 2009; 284:29320–29325. [PubMed: 19713212]
9. Cucu D, Simaels J, Van Driessche W, Zeiske W. External Ni²⁺ and ENaC in A6 cells: Na⁺ current stimulation by competition at a binding site for amiloride and Na⁺. *J Membr Biol.* 2003; 194:33–45. [PubMed: 14502441]
10. Sheng S, Perry CJ, Kleyman TR. Extracellular Zn²⁺ activates epithelial Na⁺ channels by eliminating Na⁺ self-inhibition. *J Biol Chem.* 2004; 279:31687–31696. [PubMed: 15145943]
11. Chraibi A, Schnizler M, Clauss W, Horisberger JD. Effects of 8-cpt-cAMP on the epithelial sodium channel expressed in *Xenopus* oocytes. *J Membr Biol.* 2001; 183:15–23. [PubMed: 11547348]
12. Nie HG, Zhang W, Han DY, Li QN, Li J, Zhao RZ, Su XF, Peng JB, Ji HL. 8-pCPT-cGMP stimulates alphatetagamma-ENaC activity in oocytes as an external ligand requiring specific nucleotide moieties. *Am J Physiol Renal Physiol.* 2010; 298:F323–334. [PubMed: 20007351]
13. Chraibi A, Horisberger JD. Stimulation of epithelial sodium channel activity by the sulfonyleurea glibenclamide. *J Pharmacol Exp Ther.* 1999; 290:341–347. [PubMed: 10381797]
14. Roch A, Shlyonsky V, Goolaerts A, Mies F, Sariban-Sohraby S. Halothane directly modifies Na⁺ and K⁺ channel activities in cultured human alveolar epithelial cells. *Mol Pharmacol.* 2006; 69:1755–1762. [PubMed: 16399849]
15. Li JH, Kau ST. Bumetanide stimulation of sodium permeability of the apical membrane of toad urinary bladder. *J Pharmacol Exp Ther.* 1988; 246:980–985. [PubMed: 2843638]
16. Lu M, Echeverri F, Kalabat D, Laita B, Dahan DS, Smith RD, Xu H, Staszewski L, Yamamoto J, Ling J, Hwang N, Kimmich R, Li P, Patron E, Keung W, Patron A, Moyer BD. Small molecule activator of the human epithelial sodium channel. *J Biol Chem.* 2008; 283:11981–11994. [PubMed: 18326490]
17. Chraibi A, Horisberger JD. Na self inhibition of human epithelial Na channel: temperature dependence and effect of extracellular proteases. *J Gen Physiol.* 2002; 120:133–145. [PubMed: 12149276]
18. Cucu D, Simaels J, Eggermont J, Van Driessche W, Zeiske W. Opposite effects of Ni²⁺ on *Xenopus* and rat ENaCs expressed in *Xenopus* oocytes. *Am J Physiol Cell Physiol.* 2005; 289:C946–958. [PubMed: 15944207]
19. Maarouf AB, Sheng N, Chen J, Winarski KL, Okumura S, Carattino MD, Boyd CR, Kleyman TR, Sheng S. Novel determinants of epithelial sodium channel gating within extracellular thumb domains. *J Biol Chem.* 2009; 284:7756–7765. [PubMed: 19158091]
20. Bianchi L, Driscoll M. Protons at the gate: DEG/ENaC ion channels help us feel and remember. *Neuron.* 2002; 34:337–340. [PubMed: 11988165]
21. Lingueglia E, Deval E, Lazdunski M. FMRFamide-gated sodium channel and ASIC channels: a new class of ionotropic receptors for FMRFamide and related peptides. *Peptides.* 2006; 27:1138–1152. [PubMed: 16516345]
22. Renaud S, Allache R, Chraibi C. Ile481 from the guinea pig alpha-subunit plays a major role in the activation of ENaC by cpt-cAMP. *Cell Physiol Biochem.* 2008; 22:101–108. [PubMed: 18769036]

23. Tamba K, Oh YS, Tucker JK, Quick MW, Warnock DG. Epithelial sodium channels expressed in *Xenopus* oocytes are activated by cyclic-AMP. *Clin Exp Nephrol.* 2002; 6:195–201.
24. Chen L, Song W, Davis IC, Shrestha K, Schwiebert E, Sullender WM, Matalon S. Inhibition of Na⁺ transport in lung epithelial cells by respiratory syncytial virus infection. *Am J Respir Cell Mol Biol.* 2009; 40:588–600. [PubMed: 18952569]
25. Bubien JK, Ismailov, Berdiev BK, Cornwell T, Lifton RP, Fuller CM, Achard JM, Benos DJ, Warnock DG. Liddle's disease: abnormal regulation of amiloride-sensitive Na⁺ channels by beta-subunit mutation. *Am J Physiol.* 1996; 270:C208–213. [PubMed: 8772446]
26. Bubien JK, Cornwell T, Bradford AL, Fuller CM, DuVall MD, Benos DJ. Alpha-adrenergic receptors regulate human lymphocyte amiloride-sensitive sodium channels. *Am J Physiol.* 1998; 275:C702–710. [PubMed: 9730954]
27. Bubien JK, Watson B, Khan MA, Langloh AL, Fuller CM, Berdiev B, Tousson A, Benos DJ. Expression and regulation of normal and polymorphic epithelial sodium channel by human lymphocytes. *J Biol Chem.* 2001; 276:8557–8566. [PubMed: 11113130]
28. Sheng S, Perry CJ, Kleyman TR. External nickel inhibits epithelial sodium channel by binding to histidine residues within the extracellular domains of alpha and gamma subunits and reducing channel open probability. *J Biol Chem.* 2002; 277:50098–50111. [PubMed: 12397059]
29. Sheng S, Maarouf AB, Bruns JB, Hughey RP, Kleyman TR. Functional role of extracellular loop cysteine residues of the epithelial Na⁺ channel in Na⁺ self-inhibition. *J Biol Chem.* 2007; 282:20180–20190. [PubMed: 17522058]
30. Kleyman TR, Carattino MD, Hughey RP. ENaC at the Cutting Edge: Regulation of Epithelial Sodium Channels by Proteases. *J Biol Chem.* 2009; 284:20447–20451. [PubMed: 19401469]
31. Rossier BC, Stutts MJ. Activation of the epithelial sodium channel (ENaC) by serine proteases. *Annu Rev Physiol.* 2009; 71:361–379. [PubMed: 18928407]
32. Planes C, Caughey GH. Regulation of the epithelial Na⁺ channel by peptidases. *Curr Top Dev Biol.* 2007; 78:23–46. [PubMed: 17338914]
33. Lingueglia E, Voilley N, Waldmann R, Lazdunski M, Barbry P. Expression cloning of an epithelial amiloride-sensitive Na⁺ channel. A new channel type with homologies to *Caenorhabditis elegans* degenerins. *FEBS Lett.* 1993; 318:95–99. [PubMed: 8382172]
34. Ji HL, Parker S, Langloh AL, Fuller CM, Benos DJ. Point mutations in the post-M2 region of human alpha-ENaC regulate cation selectivity. *Am J Physiol Cell Physiol.* 2001; 281:C64–74. [PubMed: 11401828]
35. Su X, Li Q, Shrestha K, Cormet-Boyaka E, Chen L, Smith PR, Sorscher EJ, Benos DJ, Matalon S, Ji HL. Interregulation of proton-gated Na⁽⁺⁾ channel 3 and cystic fibrosis transmembrane conductance regulator. *J Biol Chem.* 2006; 281:36960–36968. [PubMed: 17012229]
36. Han DY, Nie HG, Gu X, Nayak RC, Su XF, Fu J, Chang Y, Rao V, Ji HL. K⁺ channel openers restore verapamil-inhibited lung fluid resolution and transepithelial ion transport. *Respir Res.* 2010; 11:65. [PubMed: 20507598]
37. Ji HL, Su XF, Kedar S, Li J, Barbry P, Smith PR, Matalon S, Benos DJ. Delta-subunit confers novel biophysical features to alpha beta gamma-human epithelial sodium channel (ENaC) via a physical interaction. *J Biol Chem.* 2006; 281:8233–8241. [PubMed: 16423824]
38. Bangel-Ruland N, Sobczak K, Christmann T, Kentrup D, Langhorst H, Kusche-Vihrog K, Weber WM. Characterization of the epithelial sodium channel delta-subunit in human nasal epithelium. *Am J Respir Cell Mol Biol.* 42:498–505. [PubMed: 19520916]
39. Nie HG, Chen L, Han DY, Li J, Song WF, Wei SP, Fang XH, Gu X, Matalon S, Ji HL. Regulation of epithelial sodium channels by cGMP/PKGII. *J Physiol.* 2009; 587:2663–2676. [PubMed: 19359370]
40. Berdiev BK, Karlson KH, Jovov B, Ripoll PJ, Morris R, Loffing-Cueni D, Halpin P, Stanton BA, Kleyman TR, Ismailov. Subunit stoichiometry of a core conduction element in a cloned epithelial amiloride-sensitive Na⁺ channel. *Biophys J.* 1998; 75:2292–2301. [PubMed: 9788924]
41. Dijkink L, Hartog A, van Os CH, Bindels RJ. The epithelial sodium channel (ENaC) is intracellularly located as a tetramer. *Pflugers Arch.* 2002; 444:549–555. [PubMed: 12136275]
42. Firsov D, Gautschi I, Merillat AM, Rossier BC, Schild L. The heterotetrameric architecture of the epithelial sodium channel (ENaC). *Embo J.* 1998; 17:344–352. [PubMed: 9430626]

43. Kosari F, Sheng S, Li J, Mak DO, Foskett JK, Kleyman TR. Subunit stoichiometry of the epithelial sodium channel. *J Biol Chem*. 1998; 273:13469–13474. [PubMed: 9593680]
44. Snyder PM, Cheng C, Prince LS, Rogers JC, Welsh MJ. Electrophysiological and biochemical evidence that DEG/ENaC cation channels are composed of nine subunits. *J Biol Chem*. 1998; 273:681–684. [PubMed: 9422716]
45. Staruschenko A, Medina JL, Patel P, Shapiro MS, Booth RE, Stockand JD. Fluorescence resonance energy transfer analysis of subunit stoichiometry of the epithelial Na⁺ channel. *J Biol Chem*. 2004; 279:27729–27734. [PubMed: 15096495]
46. Jasti J, Furukawa H, Gonzales EB, Gouaux E. Structure of acid-sensing ion channel 1 at 1.9 Å resolution and low pH. *Nature*. 2007; 449:316–323. [PubMed: 17882215]
47. Caldwell RA, Boucher RC, Stutts MJ. Neutrophil elastase activates near-silent epithelial Na⁺ channels and increases airway epithelial Na⁺ transport. *Am J Physiol Lung Cell Mol Physiol*. 2005; 288:L813–819. [PubMed: 15640288]
48. Caldwell RA, Boucher RC, Stutts MJ. Serine protease activation of near-silent epithelial Na⁺ channels. *Am J Physiol Cell Physiol*. 2004; 286:C190–194. [PubMed: 12967915]
49. Svenningsen P, Bistrup C, Friis UG, Bertog M, Haerteis S, Krueger B, Stubbe J, Jensen ON, Thiesson HC, Uhrenholt TR, Jespersen B, Jensen BL, Korbmacher C, Skott O. Plasmin in nephrotic urine activates the epithelial sodium channel. *J Am Soc Nephrol*. 2009; 20:299–310. [PubMed: 19073825]
50. Svenningsen P, Uhrenholt TR, Palarasah Y, Skjodt K, Jensen BL, Skott O. Prostatin-dependent activation of epithelial Na⁺ channels by low plasmin concentrations. *Am J Physiol Regul Integr Comp Physiol*. 2009; 297:R1733–1741. [PubMed: 19793956]
51. Passero CJ, Mueller GM, Rondon-Berrios H, Tofovic SP, Hughey RP, Kleyman TR. Plasmin activates epithelial Na⁺ channels by cleaving the gamma subunit. *J Biol Chem*. 2008; 283:36586–36591. [PubMed: 18981180]
52. McMahon B, Kwaan HC. The plasminogen activator system and cancer. *Pathophysiol Haemost Thromb*. 2008; 36:184–194. [PubMed: 19176991]
53. Shetty S, Idell S. Post-transcriptional regulation of urokinase mRNA. Identification of a novel urokinase mRNA-binding protein in human lung epithelial cells in vitro. *J Biol Chem*. 2000; 275:13771–13779. [PubMed: 10788498]
54. Shlyonsky V, Goolaerts A, Mies F, Naeije R. Electrophysiological characterization of rat type II pneumocytes in situ. *Am J Respir Cell Mol Biol*. 2008; 39:36–44. [PubMed: 18276797]
55. Vetter AE, O'Grady SM. Mechanisms of electrolyte transport across the endometrium. I. Regulation by PGF₂ alpha and cAMP. *Am J Physiol*. 1996; 270:C663–672. [PubMed: 8779933]
56. Frindt G, Silver RB, Windhager EE, Palmer LG. Feedback regulation of Na channels in rat CCT. III. Response to cAMP. *Am J Physiol*. 1995; 268:F480–489. [PubMed: 7900848]
57. Segal A, Cucu D, Van Driessche W, Weber WM. Rat ENaC expressed in *Xenopus laevis* oocytes is activated by cAMP and blocked by Ni(2+). *FEBS Lett*. 2002; 515:177–183. [PubMed: 11943217]
58. Xie Y, Schafer JA. Inhibition of ENaC by intracellular Cl⁻ in an MDCK clone with high ENaC expression. *Am J Physiol Renal Physiol*. 2004; 287:F722–731. [PubMed: 15161604]
59. Matulef K, Zagotta WN. Cyclic nucleotide-gated ion channels. *Annu Rev Cell Dev Biol*. 2003; 19:23–44. [PubMed: 14570562]

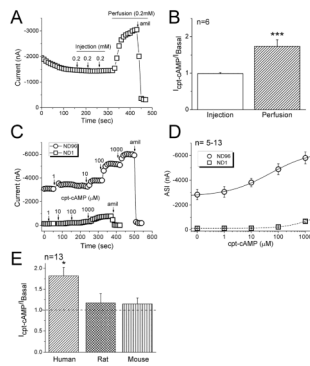


Figure 1.

Activation of heterologous $\alpha\beta\gamma$ ENaC activity by cpt-cAMP. **A.** Representative current trace showing the effects of microinjected and perfused cpt-cAMP on amiloride (amil) inhibitable current associated with human $\alpha\beta\gamma$ ENaC. Holding potential, -100 mV. **B.** The ratio of the current levels recorded after and before cpt-cAMP application ($I_{cpt-cAMP}/I_{Basal}$). Paired t-test, *** $P<0.001$. $n=6$. **C.** Representative current traces showing the responses to a variety of cpt-cAMP concentrations in oocytes bathed with regular ND96 (circle) or low Na⁺ solution, ND1 (1 mM Na⁺, square). **D.** Dose-response curves of amiloride-sensitive currents (ASI). The solid (ND96) and dashed lines (ND1) were created by fitting the current data with the Hill equation to compute the EC_{50} values. $n\sim 13$. **E.** Species diversity in responses to cpt-cAMP among human, rat, and mouse $\alpha\beta\gamma$ ENaCs. $n=13$. * $P<0.05$.

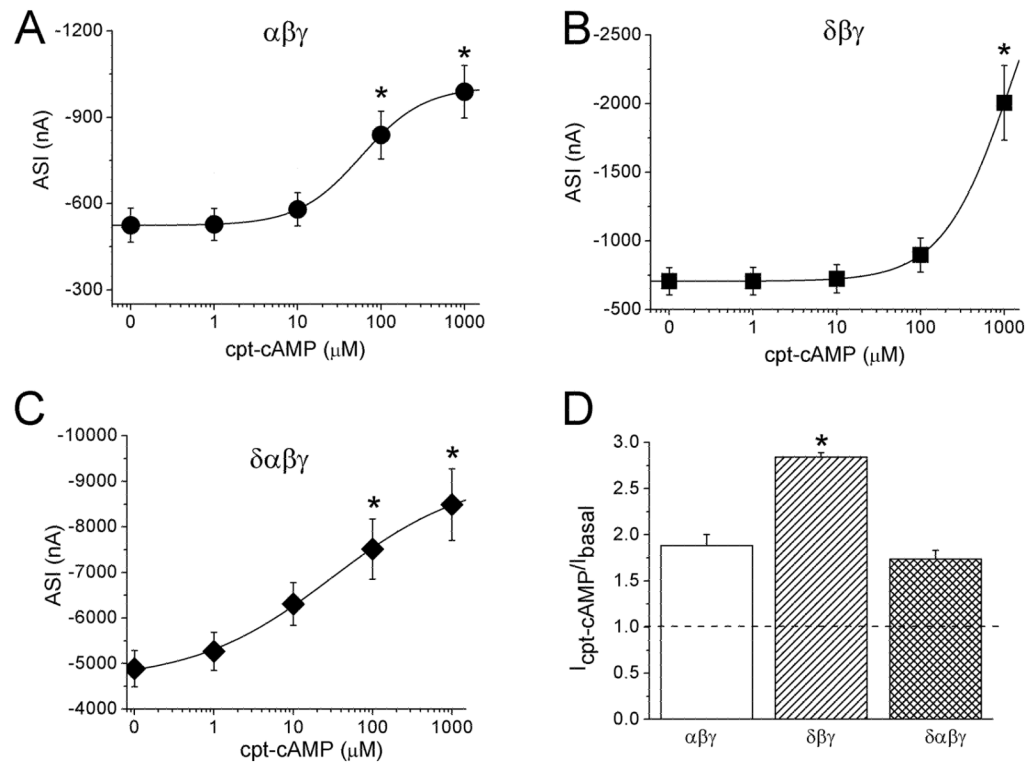


Figure 2.

Divergent responses of human $\delta\beta\gamma$, $\alpha\beta\gamma$, and $\delta\alpha\beta\gamma$ ENaCs to cpt-cAMP. A–C. Dose response curves of $\alpha\beta\gamma$ (A), $\delta\beta\gamma$ (B), and $\delta\alpha\beta\gamma$ ENaC (C). Average amiloride-sensitive currents (ASI) measured at the cpt-cAMP ranging from 0 to 1 mM were fitted with the Hill equation. $n=8-9$. * $P<0.05$ vs that at 0 mM cpt-cAMP. Paired t-test. D. Current ratio showing the responses to cpt-cAMP ($I_{\text{cpt-cAMP}}/I_{\text{Basal}}$). * $P<0.05$ vs $\alpha\beta\gamma$ ENaC.

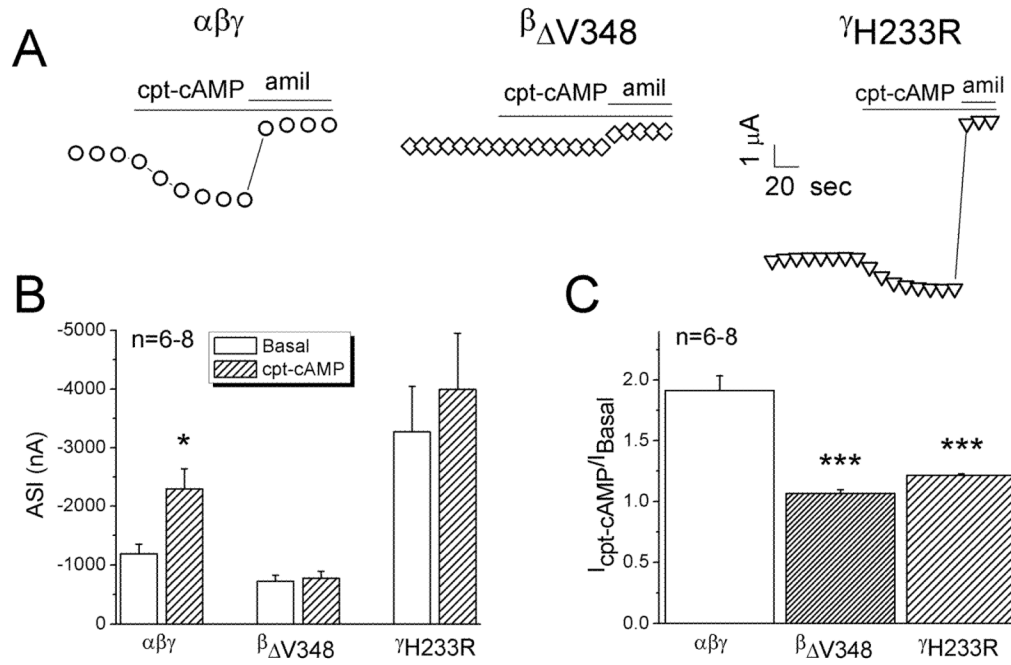


Figure 3.

Responses of “loss-of-self-inhibition” mutants to cpt-cAMP. *A.* Representative current traces of wild type $\alpha\beta\gamma$, $\alpha\beta_{\Delta V348}\gamma$, and $\alpha\beta_{\gamma H233R}$ channels. *B.* Amiloride-sensitive Na^+ currents (ASI) at -100 mV in the absence (Basal) and presence of cpt-cAMP. * $P < 0.05$ vs Basal levels. Paired t-test. $n = 6-8$. *C.* Current ratio. *** $P < 0.001$ vs $\alpha\beta\gamma$ ENaC. Two-sample t-test.

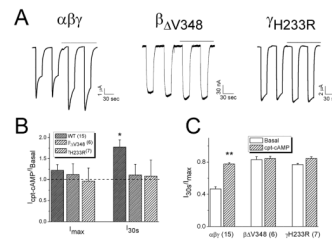


Figure 4.

Loss of responses to cpt-cAMP in cells expressing “loss-of-self-inhibition” mutants. *A.* Representative current traces for $\alpha\beta\gamma$, $\alpha\beta_{\Delta V348}\gamma$, and $\alpha\beta\gamma_{H233R}$. Horizontal lines above the traces indicate the application of cpt-cAMP. *B.* Alteration of currents by cpt-cAMP. * $P < 0.05$ vs that in the absence of drug ($I_{cpt-cAMP}/I_{Basal}$). Dashed line is the basal level. *C.* Current ratio of measurements at 30 sec (I_{30s}) over peak levels (I_{max}) post switching of bath solution from ND1 to ND96 medium. ** $P < 0.01$ vs Basal.

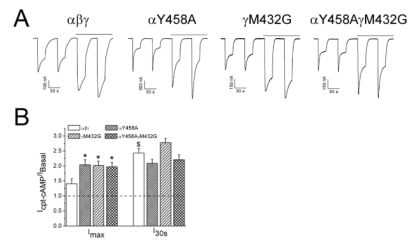


Figure 5. Effects of cpt-cAMP on “gain-of-self-inhibition” mutants. *A.* Representative self-inhibition traces for $\alpha\beta\gamma$, $\alpha Y458A\beta\gamma$, $\alpha\beta\gamma M432G$, and $\alpha Y458A\beta\gamma M432G$. *B.* Up-regulation of currents by cpt-cAMP. *P < 0.05 vs $\alpha\beta\gamma$ and \$P < 0.05 vs I_{max} .

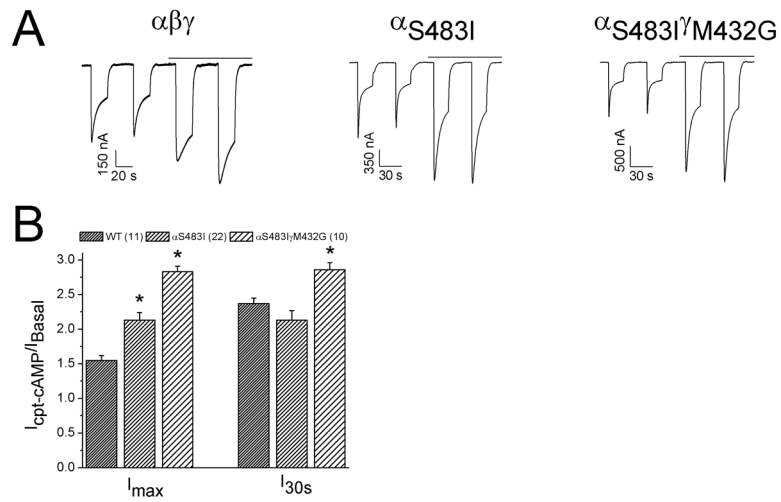


Figure 6. Response of cpt-cAMP enhancing mutant ($\alpha S483I\beta\gamma$). **A.** Representative self-inhibition traces for $\alpha\beta\gamma$, $\alpha S483I\beta\gamma$, and $\alpha S483I\beta\gamma M432G$. **B.** I_{30s}/I_{max} ratio. * $P < 0.05$ vs $\alpha\beta\gamma$. Numbers in brackets are examined cells.

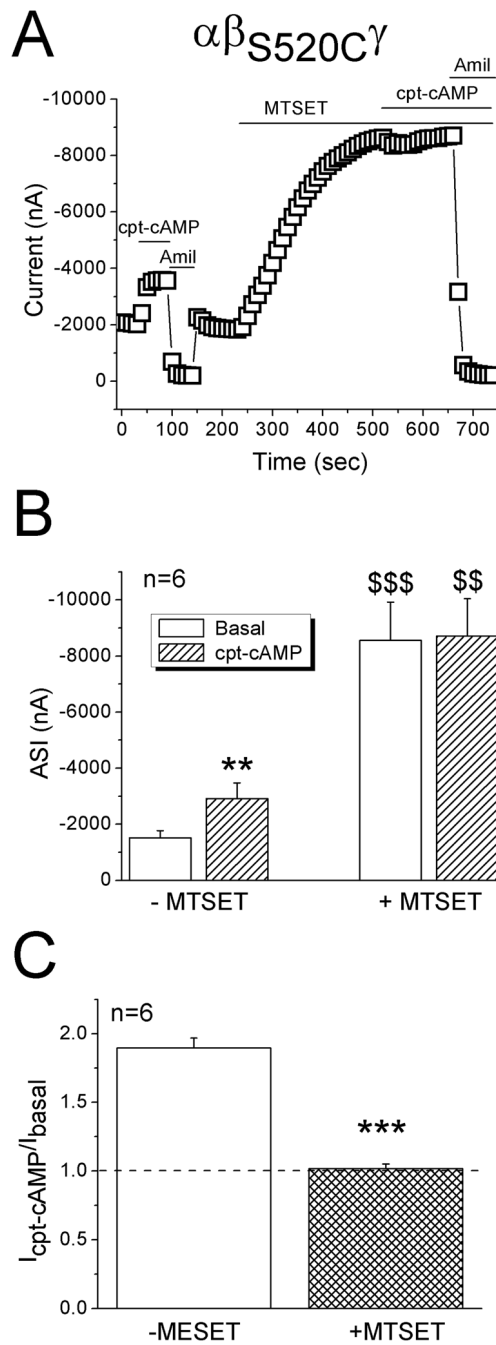


Figure 7. Effects of cpt-cAMP on a degenerin mutant ($\alpha\beta_{S520C}\gamma$). **A.** Representative current trace at -100 mV showing the diverse effects of cpt-cAMP before and after MTSET. **B.** Average ENaC currents (ASI). ** $P < 0.01$ vs Basal; \$\$ and \$\$\$ $P < 0.01$ and 0.001 , respectively, vs those in the absence of MTSET. **C.** Current ratio of cpt-cAMP activated and basal levels. *** $P < 0.001$.

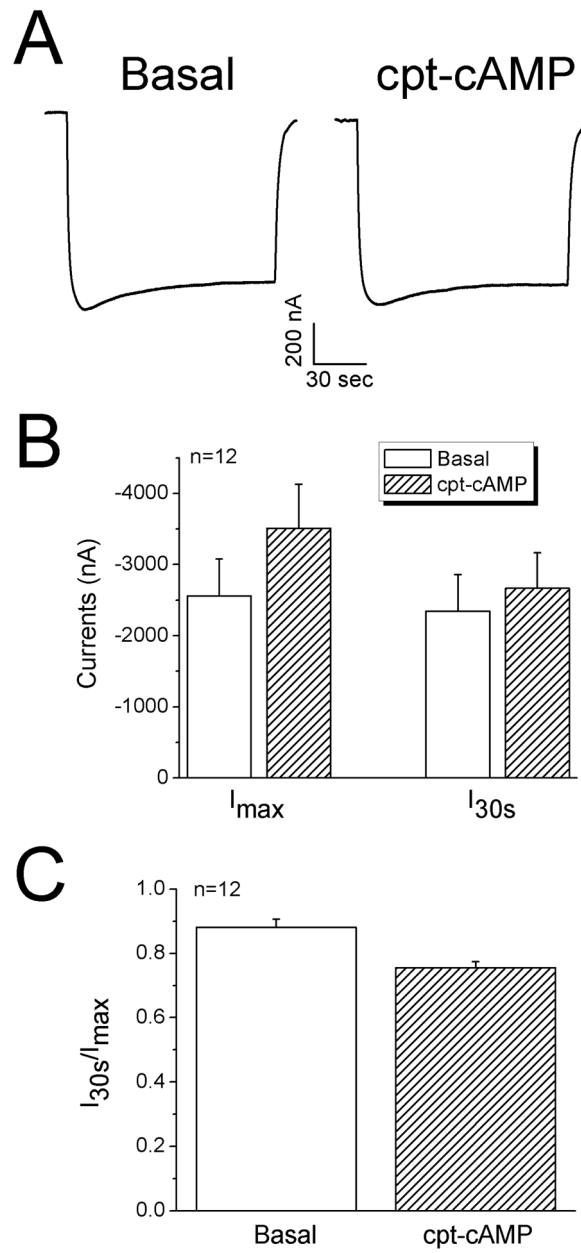


Figure 8. Regulation of proteolytically cleaved ENaC by cpt-cAMP. **A.** Representative current trace from an oocyte preincubated with plasmin (10 μ g/ml) for 3 hrs in OR-2 medium. **B.** Average increase in both I_{max} and I_{30s} levels. **C.** Current ratio. n=12.

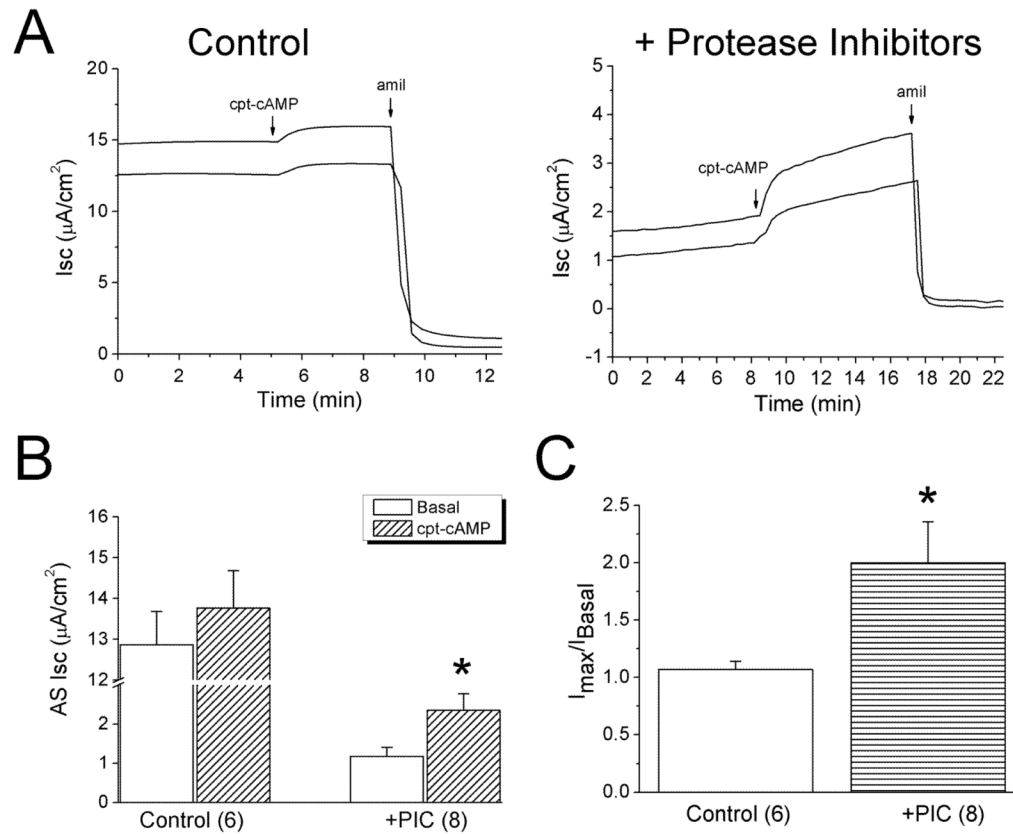


Figure 9. Relief of self-inhibition by protease inhibitors in human lung epithelial cells (H441 cells). **A.** Transepithelial short-circuit currents (I_{sc}) showing the effects of cpt-cAMP (0.5 mM) in monolayers preincubated with protease inhibitor cocktail (right) and controls (left). **B.** Average amiloride-sensitive (AS) currents in untreated (Control) and cells pretreated with protease inhibitor cocktail (PIC). $n=6-8$. $*P<0.05$ vs Basal. **C.** Stimulating potency of cpt-cAMP (I_{max}/I_{Basal}). $n=6-8$. $*P<0.05$ vs Controls.